SOILS AND FOUNDATIONS Vol. 32, No. 3, 156-173, Sept. 1992
Japanese Society of Soil Mechanics and Foundation Engineering

# A PORE PRESSURE MODEL FOR CYCLIC STRAINING OF CLAY

NEVEN MATASOVIĆ[i] and MLADEN VUCETIC[ii]

## ABSTRACT

The paper focuses on the development and modelling of residual cyclic pore water pressure, $u$, in clay during undrained cyclic strain-controlled loading. Data obtained from a series of NGI type cyclic simple shear tests were employed. In addition to the amplitude of cyclic shear strain, $\gamma_c$, the number of cycles, $N$, and the overconsolidation ratio, $OCR$, a new component is incorporated in the conventional characterization of $u$. This new component is the volumetric threshold shear strain, $\gamma_{tv}$, of clayey soils, below which for all practical purposes $u$ does not develop. The lack of understanding of complex clay microstructure and the associated interaction between clay particles during cyclic shearing makes the modelling of $u$ in a manner other than curve fitting rather difficult. This is especially true in regard to the development of negative $u$ in overconsolidated clays. A model based on the systematic curve fitting of the pore pressure data expressed in terms of $\gamma_c$, $\gamma_{tv}$, $N$ and $OCR$ is presented. The possibilities of the incorporation of such a model into existing numerical tools for simulation of the seismic and ocean wave loading response of natural soil deposits are briefly discussed as well.

**Key words:** clay, cyclic, dynamic, modelling, pore pressure, simple shear, threshold strain (**IGC**: D7/E8)

## 1. INTRODUCTION

When a saturated soil deposit is subjected to cyclic shear, the pore water pressure changes. Because of its effects on the cyclic stiffness and strength of the soil, such variation of pore water pressure is an important component of the cyclic characterization of soil deposits. The phenomenon of cyclic pore water pressure buildup in sands and sandy soils has been extensively studied, mainly in connection with the mechanism of soil liquefaction (NRC, 1985). The cyclic pore water pressure generation in clays, although also systematically studied by a number of researchers, has not received so much attention. The reason might be considerably smaller cyclic pore water pressures in clays than in sands, *i.e.*, smaller earthquake damages which can be attributed to the cyclic pore pressure development. However, the phenomenon of the generation of cyclic pore water pressures in clay is important in connection with the seismic response and cyclic degradation of clay deposits. It is quite important in connection with the seismic response of deposits composed of layers of

[i] Research Assistant, Civil Engineering Department, University of California, Los Angeles, CA 90024-1593, USA.
[ii] Assistant Professor, ditto.
Manuscript was received for review on July 15, 1991.
Written discussions on this paper should be submitted before April 1, 1993, to the Japanese Society of Soil Mechanics and Foundation Engineering, Sugayama Bldg. 4F, Kanda Awaji-cho 2-23, Chiyoda-ku, Tokyo 101, Japan. Upon request the closing date may be extended one month.

saturated sands and clays and it is a very important component of the cyclic response of clay deposits below offshore structures.

The pore water pressure is varying during each cycle of loading or shear straining, $N$, regardless of the level of the applied cyclic shear stress amplitude, $\tau_c$, or the cyclic shear strain amplitude, $\gamma_c$. However, when the applied amplitude $\tau_c$ or $\gamma_c$ is smaller than a certain threshold value, no permanent pore water pressure remains after the cyclic loading or shear straining has stopped. In the same way, when $\tau_c$ or $\gamma_c$ larger than such thresholds are applied, a permanent pore water pressure remains after the cyclic straining has stopped. These threshold values are called here the volumetric threshold cyclic shear stress and the volumetric threshold cyclic shear strain, and are denoted by $\tau_{tv}$ and $\gamma_{tv}$ respectively[1]. The pore water pressure remaining permanently is termed the residual cyclic pore water pressure and is denoted by $u$.

While $u$ is always positive in sands and normally consolidated, NC, clays, it may be negative in some overconsolidated, OC, clays, as revealed by several studies (NGI, 1975; Andersen et al., 1980; Matsui et al., 1980; Vucetic et al., 1985; Vucetic, 1988; Tan and Vucetic, 1989). In general, it has been observed that higher overconsolidation ratio, $OCR$, causes larger negative $u$ with $N$ in the beginning of cyclic shearing. Such complex behavior makes the cyclic pore water pressure response of clays rather difficult to model. Accordingly, while the excess cyclic pore water pressure in sands and NC clays is relatively easy to describe in terms of $\tau_c$ or $\gamma_c$ and the associated $N$, the cyclic pore water pressure response of OC clays is more difficult to describe and explain.

Because of its strong dependence on $OCR$, it is evident that the pore water pressure response of OC clays depends strongly on clay loading history and changes of clay microstructure during cyclic loading or cyclic shear straining. Hypotheses regarding such rather complex microstructural mechanisms which cause and govern the development of negative $u$ in OC clays have already been made (Dobry and Vucetic, 1987), but the phenomenon has not been fully explained.

The study described here focuses on the residual cyclic pore water pressure generation in clay during, so called, cyclic strain-controlled test, in which the amplitude of $\gamma_c$ is maintained constant. Besides $u$, $\gamma_c$, $N$ and $OCR$, a new component of this cyclic shear strain approach is the volumetric threshold shear strain, $\gamma_{tv}$, below which $u$ does not develop or is negligibly small, regardless of $N$. Accordingly, in this study an effort was made to develop a model for a mathematical description of the development of $u$ in the specimen subjected to cyclic strain-controlled shearing in terms of $\gamma_c$, $\gamma_{tv}$, $OCR$ and $N$. The procedure is based on the curve fitting of the cyclic pore pressure data in a systematic manner. The possibilities of incorporating the model into existing numerical tools for simulation of the seismic and ocean wave loading response of natural soil deposits are discussed as well.

## 2. CYCLIC PORE WATER PRESSURE BEHAVIOR OF DIFFERENT SOILS

The cyclic loading caused by earthquake shaking, ocean wave storms and some other sources leads to the tendency toward a volume change of the soil, *i.e.*, the tendency toward either compaction or dilation. In cases where the soil profile consists of dry cohesionless granular materials, the cyclic loading will cause compaction (Silver and Seed, 1971; Youd, 1972). If such soils are fully saturated, the cyclic loading will result in the development of the excess pore water pressures, sometimes of sufficient magnitude to cause liquefaction of the soil (NRC, 1985). If drainage is provided, the settlement of saturated cohesionless soils will also occur during and after cyclic loading.

In partially saturated clayey soils the settle-

[1] The term "volumetric threshold shear strain" and the notation $\gamma_{tv}$ have been adopted at the 10th European Conf. on Soil Mechanics and Foundation Engineering held in 1991 in Florence, Italy, by a group of European and U.S. researchers who are dealing with Soil Dynamics.

ment during cyclic loading will occur just like in the dry cohesionless soils. Under the same cyclic loading conditions, in fully saturated clayey soils residual pore water pressures will develop. The excess pore water pressures induced by such cyclic loading can also be accompanied by the settlement of the soil during and especially after the cyclic loading. However, the settlement during relatively short cyclic loading, such as earthquake shaking, is usually negligible. This is because the permeability of clay is low and there is not enough time for the water to drain out. In any case, it is evident that cyclic pore water pressure generation and settlement of cohesionless and cohesive soils are conceptually interrelated in a similar manner.

The analogy between the cyclic settlement and cyclic pore water pressure generation just described, which applies to both cohesionless and clayey soils, will be used in the following sub-sections to discuss the existence and approximate magnitude of $\gamma_{tv}$ in clays.

### *2.1 Analogy between Settlement of Dry Sands and Pore Pressure Buildup in Fully Saturated Sands*

Figure 1 shows the compaction of a dry sand during strain-controlled cyclic direct simple shear test (CyDSS). These results, obtained by Youd (1972), and similar tests by Silver and Seed (1971) and Pyke et al. (1975) have led to the following conclusions: (i) The change in density and associated settlement are a function mainly of the initial relative density of the sand, $D_r$, or the associated void ratio, $e$, and the value of $N$ and $\gamma_c$ applied. (ii) The change in density is independent of the frequency of loading. (iii) The change in density is independent of the vertical effective consolidation stress, $\sigma'_{vc}$. (iv) There is a threshold value of the cyclic shear strain $\gamma_{tv} \cong 10^{-2}\%$, as suggested by dashed lines in Fig. 1, below which no change in volume occurs.

As shown by Dobry et al. (1982) and depicted in Fig. 2 (NRC, 1985), the concept of volumetric threshold shear strain, $\gamma_{tv}$, in sands is not only of particular interest for settlement studies, but also for the cyclic pore water pressure buildup studies. In fact, in saturated cohesionless soils sheared in undrained conditions residual cyclic pore water pressure, $u$, develops as a result of the tendency of the soil to densify, *i.e.*, to decrease in volume. It is therefore not surprising that the experimental evidence by numerous authors, which is syn-

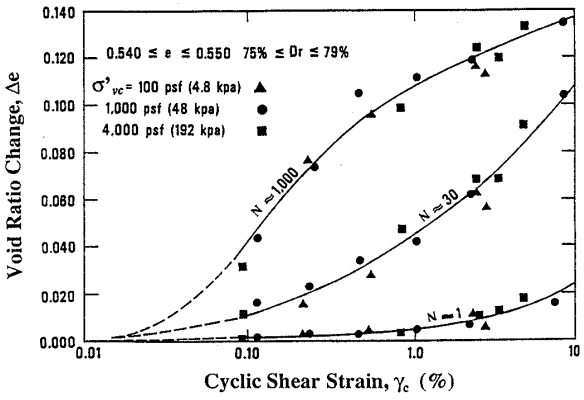


**Fig. 1. Compaction (void ratio change) of dry sand during cyclic strain-controlled direct simple shear test (Youd, 1972)**

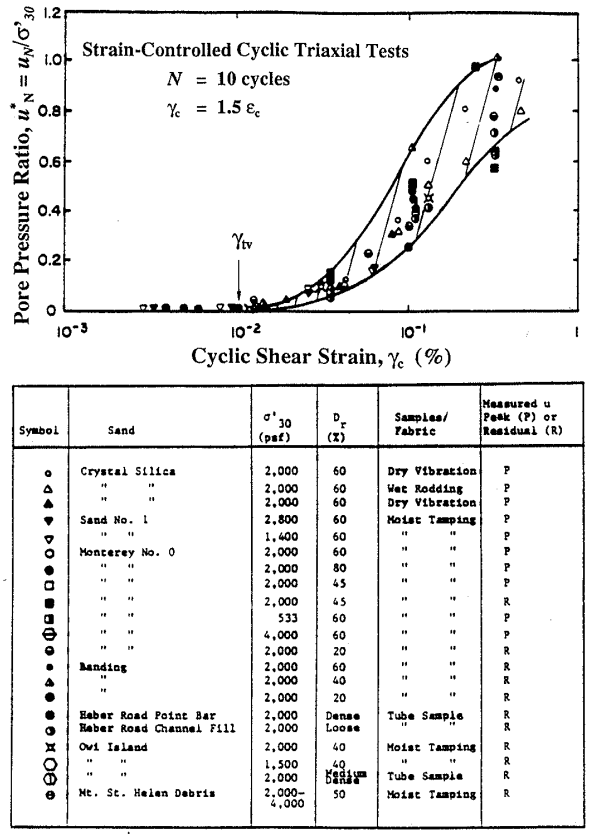


| Symbol | Sand | σ'30 (psf) | DF (%) | Samples/ Fabric | Measured u Peak (P) or Residual (R) |
|---|---|---|---|---|---|
| o | Crystal Silica | 2,000 | 60 | Dry Vibration | P |
| △ | " " | 2,000 | 60 | Wet Rodding | P |
| ▲ | " " | 2,000 | 60 | Dry Vibration | P |
| ▼ | Sand No. 1 | 2,800 | 60 | Moist Tamping | P |
| ▽ | " " | 1,400 | 60 | " " | P |
| ○ | Monterey No. 0 | 2,000 | 60 | " " | P |
| ● | " " | 2,000 | 80 | " " | P |
| □ | " " | 2,000 | 45 | " " | P |
| ■ | " " | 2,000 | 45 | " " | R |
| ⊕ | " " | 533 | 60 | " " | P |
| ⊗ | " " | 4,000 | 60 | " " | P |
| ◆ | " " | 2,000 | 20 | " " | R |
| • | Banding | 2,000 | 60 | " " | R |
| ◆ | " | 2,000 | 40 | " " | R |
| ● | " | 2,000 | 20 | " " | R |
| ● | Haber Road Point Bar | 2,000 | Dense | Tube Sample | R |
| ⊙ | Haber Road Channel Fill | 2,000 | Loose | " " | R |
| ⊠ | Owl Island | 2,000 | 40 | Moist Tamping | R |
| ⊙ | " " | 1,500 | 40 | " " | R |
| ⊙ | " " | 2,000 | Medium Dense | Tube Sample | R |
| ⊖ | Mt. St. Helen Debris | 2,000-4,000 | 50 | Moist Tamping | R |

**Fig. 2. Excess pore water pressure generation in saturated sands during cyclic strain-controlled triaxial testing (Synthesis by Dobry presented in NRC, 1985)**

thesized in Fig. 2, demonstrates the existence of the same $\gamma_{tv} \cong 10^{-2}\%$ in saturated sands, which is in this case defined as the cyclic shear strain amplitude below which no $u$ develops. It should be noted that $u$ after cycle $N$ is presented in Fig. 2 in the normalized form, $u_N^*$, with respect to the effective confining pressure, $\sigma'_{30}$. The results shown in Fig. 1 for settlement and in Fig. 2 for the excess pore water pressure generation, strongly suggest that for a variety of sands, relative densities, and effective confining pressures, neither settlement in dry sand nor noticeable pore water pressure buildup in saturated sand will occur if the cyclic shear strain, $\gamma_c$, is less than the volumetric threshold shear strain of $\gamma_{tv} \cong 10^{-2}\%$.

Dobry and Swiger (1979) have explained the existence of the value of $\gamma_{tv} \cong 10^{-2}\%$ in sands on the basis of a simple model consisting of an array of quartz spheres. The concept of $\gamma_{tv}$ has been used in practice for estimating pore water pressure buildup in silts by Stoll and Kald (1977), and for estimating the liquefaction potential of saturated sand deposits (Dobry et al., 1980). Finally, the concept of $\gamma_{tv}$ in fully saturated sands sheared in undrained conditions has been fully developed and employed in a pore pressure buildup model proposed by Dobry et al. (1985).

### 2.2 *Volumetric Threshold Shear Strain in Clays*

As opposed to sands, there are only a few studies dealing directly or indirectly with the $\gamma_{tv}$ in clays. It has been shown that $\gamma_{tv}$ in saturated sands is directly related to the $\gamma_{tv}$ in dry sands subjected to cyclic settlement. Evidence on the $\gamma_{tv}$ for settlement in partially saturated compacted clays has been obtained recently by Chu and Vucetic (1992) and is presented in Fig. 3. It can be seen that small but noticeable settlement starts at $\gamma_c \cong 0.05\%$, while the significant settlement starts to develop around $\gamma_c \cong 10^{-1}\%$. In that respect, for this particular clay $\gamma_{tv}$ for settlement is between 0.05% and 0.1%. It is believed that these threshold values of $\gamma_c$ can be linked to the $\gamma_{tv}$ signifying the beginning of the generation of $u$ in fully saturated clays. In other

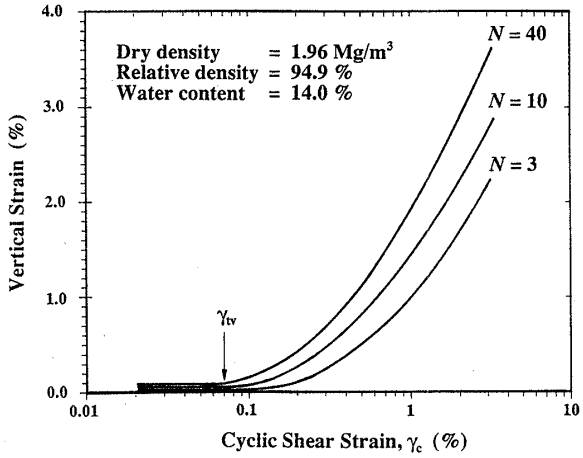


**Fig. 3. Summary of cyclic direct simple shear test results on a compacted clay (Chu and Vucetic, 1992)**

words, the analogy between the $\gamma_{tv}$ for settlement of dry sands and $\gamma_{tv}$ for pore pressure buildup in fully saturated sands can be used to discuss the $\gamma_{tv}$ in clays.

Very interesting results from a series of strain-controlled CyDSS tests on fully saturated kaolinite clay reported by Ohara and Matsuda (1987, 1988), are summarized in Figs. 4(a) and 4(b). Fig. 4(a) reveals that the pore water pressure starts to buildup up at $\gamma_c \cong 0.05\%$, but the significant change starts at $\gamma_c \cong 10^{-1}\%$. Similar observations are given in the study by Matsuda et al. (1991) based on a series of two types of irregular strain history CyDSS tests on the same kaolinite clay.

Fig. 4(b) compares the generation of the positive $u$, *i.e.*, the excess pore water pressure in the same NC and OC clay. It can be seen that in OC clay the positive pore pressure starts to build up at higher levels of $\gamma_c$. The same tendency was observed during undrained cyclic stress-controlled triaxial testing of NC and OC clay by Matsui et al. (1980). However, there are data given in the study by Ohara and Matsuda (1987, 1988), which are not reproduced here, which indicate that the generation of negative $u$ in OC clay starts at the cyclic shear strain amplitude $\gamma_c \cong 10^{-1}\%$, *i.e.*, at the same $\gamma_{tv}$ depicted in Fig. 4(a) for the positive $u$.

Based on the above evidence, a "practical" value of the volumetric threshold shear strain for clayey soils of $\gamma_{tvp} \cong 10^{-1}\%$, below which

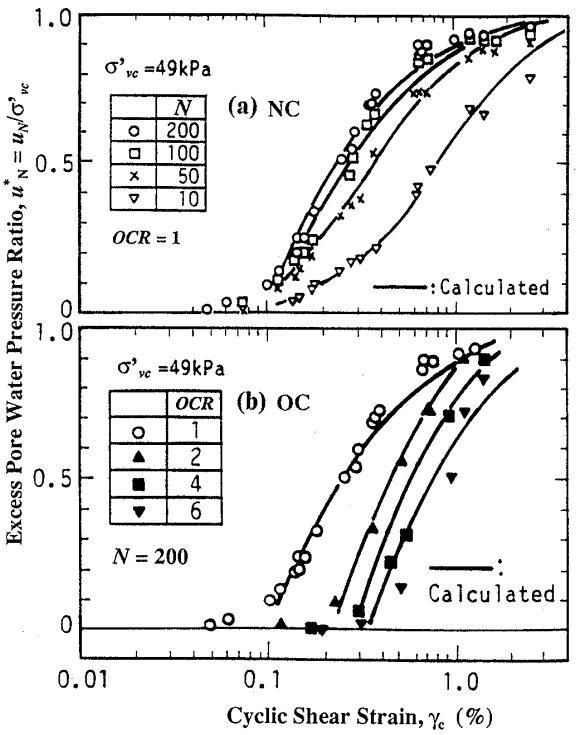


**Fig. 4. Excess pore water pressure generation in clay during cyclic strain-controlled direct simple shear test: (a) $OCR=1$; (b) $OCR=1$, 2, 4 and 6 (Ohara and Matsuda, 1987, 1988)**

neither significant positive $u$ nor significant negative $u$ occurs, can be assumed for the modelling of the generation of $u$. This value of $\gamma_{tvp}$ for clays is approximate, until more experimental data becomes available, and it is also selected based on a relationsthip between the $\gamma_{tvp}$ and the plasticity index, $PI$, developed recently (Vucetic, 1991). It should be noted at this point that the existence of $\gamma_{tvp}$ in clays has not been explained theoretically, as was done for sands by Dobry and Swiger (1979). The authors believe that an explanation for such a higher value of $\gamma_{tvp}$ in clays than in sands lies in the more flexible electrical bonds between clay particles than are the contacts between sand grains. In other words, the behavior of clay is governed by the effects that cyclic straining has on the clay microstructure, which by itself is quite complex. Further studies with a focus on the associated microstructural mechanisms are needed to explain this phenomenon.

### *2.3 Generation of Residual Cyclic Pore Water Pressure*

The generation of $u$ in saturated cohesionless soils has been extensively studied, primarily in connection with liquefaction investigations. Most of the laboratory studies have been conducted using cyclic stress-controlled tests, which historically came first. Results and conclusions have been summarized by Seed (1979) and in NRC (1985). Cyclic strain-controlled tests, on the other hand, were introduced later (Dobry et al., 1982) and have been, until recently, performed more rarely.

As far as clays are concerned, several relatively recent studies, using both cyclic stress-controlled (NGI, 1975; Andersen et al., 1980; Matsui et al., 1980; Azzouz et al., 1989) and cyclic strain-controlled testing (Vucetic et al. 1985; Ohara and Matsuda, 1987, 1988; Vucetic, 1988; Tan and Vucetic, 1989) demonstrated a rather complex nature of the clay response in a wide strain range. This particularly applies to OC clays. When OC specimens are sheared, negative $u$ may develop in the early cycles. With continued cyclic shearing, the generation of negative $u$ slowly stops, the trend is reversed, $u$ starts to increase and eventually becomes positive.

Based on the above mentioned evidence, it can be concluded that in clays the generation of the normalized $u$ after cycle $N$ depends mainly on:

(a) The applied amplitude of cyclic shear stress, $\tau_c$, or cyclic shear strain, $\gamma_c$.

(b) The number of loading or shear straining cycles, $N$.

(c) The loading history that the clay has experienced, which can be characterized by the overconsolidation ratio, $OCR$.

(d) The magnitude of $\gamma_{tv}$.

## 3. BEHAVIOR OF A SOIL ELEMENT DURING STRONG GROUND SHAKING

To use the results of laboratory tests to develop a model for assessing some aspects of the cyclic response of soil deposits, one of the main considerations is the selection of an appropriate test. The selected type of test should

simulate as closely as possible the cyclic stress-strain conditions applied on a representative soil element *in situ*. Only then will the cyclic model be useful for practical applications. This section deals briefly with the selection of a laboratory test for use in the seismic response studies. The cyclic pore pressure data from such type of test are in turn used as a data base for the development of the cyclic pore water pressure generation model.

For seismic studies, to compute the site response, assumptions must be made regarding the types of waves propagated during the earthquake. The most common assumption is that the excitation is caused by vertically propagating dilatational waves (P-waves) and shear waves (S-waves) through the soil deposits which are horizontally stratified. In such an idealized situation, the P-waves alone would produce only vertical motions which in a fully saturated soil element generate only temporary increase in pore water pressure. In other words, no $u$ in saturated soils are caused by such P-waves. Therefore, for practical purposes the effect of P-waves is very often disregarded and the problem is reduced to a one-dimensional (1-D) S-wave propagation. If such S-waves generate shear strains larger than $\gamma_{tv}$, permanent pore water pressure or volume change will develop in the soil. The behavior of an element of soil during the vertical propagation of 1-D S-waves through a saturated deposit can be rather directly simulated by the CyDSS test, or indirectly by the cyclic triaxial test. Cyclic hollow cylinder test is also appropriate, provided that lateral strains are prevented or largely reduced, just like in the CyDSS test.

In any one of the above mentioned tests the level of the applied cyclic shear strain amplitude, $\gamma_c$, is proportional to the relative movement between the particles in a single cycle, *i.e.*, proportional to the deformation of soil microstructure in a single cycle. Similarly, the number of uniform strain reversals, *i.e.*, the number of cycles, $N$, is proportional to the cumulative change of the soil microstructure during cyclic loading. These considerations, the fact that volume change depends directly on the shear deformation of the soil (Silver and Seed, 1971; Youd, 1972; Chu and Vucetic, 1990), and that the development of $u$ is the consequence of the tendency of saturated soil to change in volume, strongly suggest that $\gamma_c$ is a more fundamental parameter for studying the generation of $u$ than $\tau_c$, and that the use of the cyclic strain-controlled instead of stress-controlled tests can considerably simplify the picture of the pore water pressure development during cyclic loading.

In conclusion, the cyclic strain-controlled test data have been selected here for the modelling of the residual pore water pressure generation in clays. In particular, the data from the Norwegian Geotechnical Institute type (NGI-type) constant volume equivalent undrained CyDSS tests are employed.

## 4. REVIEW OF SOME RELEVANT PORE WATER PRESSURE GENERATION MODELS

To better understand the model for the residual cyclic pore water pressure generation in clay, developed latter herein, some relevant models, based on strain-controlled testing and developed in the past for both sands and clays, are briefly reviewed.

For sands, numerous 1-D models for the generation of $u$ due to cyclic shear straining were developed. In all of them residual pore water pressure buildup with some cumulative parameter is assumed. The cumulative parameter is either the number of shear straining cycles, $N$ (Dobry et al., 1985), damage parameter-cumulative shear deformation (Finn and Bhatia, 1981)[2], shear work (Towhata and Ishihara, 1985)[2] or normalized shear work (Moroto, 1986; Kvasnicka and Ivsic, 1991). Some of these models have a rather clear physical meaning, while the others are just based on a curve-fitting procedure.

It should be noted that only the model

[2] Applicable to both cyclic strain-controlled and stress-controlled data.

presented by Dobry et al. (1985) has practical volumetric threshold shear strain, $\gamma_{tvp}$, explicitly incorporated. In this respect the Dobry's model is similar to the model developed herein for clays. As an example, the model by Dobry et al. (1985) developed for Banding Sand is presented in Fig. 5. It should be noticed that in this particular case the practical volumetric threshold shear strain of $\gamma_{tvp}=0.017\%$ has been assumed. On the other hand, from the laboratory pore water pressure data on the same Banding Sand, which are also incorporated in Fig. 2, it is evident that the volumetric threshold shear strain $\gamma_{tv}=0.01\%$. Figure 2 shows that such an assumption of $\gamma_{tvp}$ is appropriate, because the buildup of $u$ between $\gamma_{tv}=0.01\%$ and $\gamma_{tvp}=0.017\%$ is negligible indeed[3].

However, the generation of $u$ in clay could be modelled in a similar manner as in sands only for NC clays. This is because in OC clays negative $u$ may develop, as discussed earlier. Such complex pore pressure response of OC clays makes the modelling of the generation of $u$ in clays rather difficult. Nevertheless, the models that relate $u$ to cyclic shear strain amplitude, $\gamma_c$, and the number of loading cycles, $N$, have been developed. In these models $u$ is commonly expressed in the normalized form with respect to the vertical effective consolidation stress, $\sigma'_{vc}$.

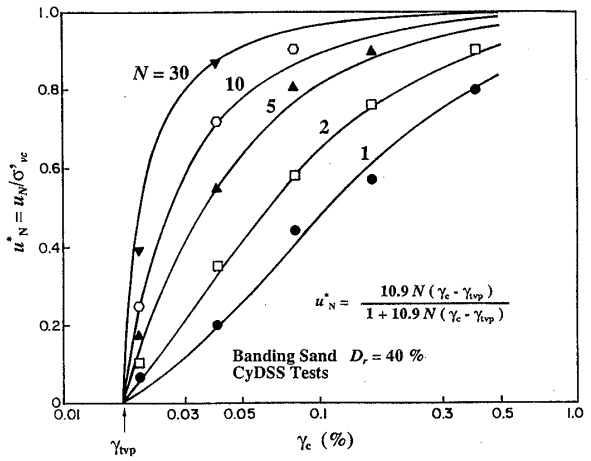


**Fig. 5. Modelling of the normalized cyclic strain-controlled pore water pressure response in sand (Dobry et al., 1985)**

Ohara et al. (1984) developed an empirical model for NC clays based on cyclic strain-controlled data. This seems to be the first such model using the cyclic strain approach. The relation between the normalized excess pore water pressure and $N$ for a constant $\gamma_c$ was formulated by utilizing a hyperbola. Consequently, only two fitting parameters are needed in such a model. Ohara and Matsuda (1987, 1988) extended the model by introducing the correction factor for the initial negative $u$ which develop when OC clay is cyclically sheared. Five empirical parameters are needed in this extended version of the model. It is interesting that the volumetric threshold shear strain in the above studies on clay was not explicitly incorporated into the models, although its existence has been indicated[4].

## 5. DEVELOPMENT OF A NEW PORE WATER PRESSURE GENERATION MODEL

The previous section reveals that it is very difficult to develop a general model for the generation of residual cyclic pore water pressure, $u$, in clay. The model based on cyclic strain-controlled test by Ohara and Matsuda (1987, 1988) is an advanced model because it incorporates practically all of the important parameters which govern the generation of $u$. However, this model does not encompass the details of the development of negative $u$ and it does not explicitly incorporate $\gamma_{tvp}$. The main reason for that may be that this model was originally developed for studying the seismic settlement of saturated clay layers (Matsuda et al. 1991), where the influence of negative $u$ is negligible.

Therefore, for 1-D studies of seismic or ocean wave loading response of natural clay deposits a more general cyclic pore water pressure generation model can be developed. The main requirements on such a model are:

(a) The model should be of the following

[3] Note that Fig. 2 shows pore water pressure buildup after 10 cycles.

[4] Defined in these studies as "minimum shear strain amplitude which produces the excess pore water pressure."

general form: $u_N^*=0$ for $\gamma_c \leq \gamma_{tvp}$ and $u_N^*=u_N^*$ ($\gamma_c$, $OCR$, $N$, $\gamma_{tvp}$) for $\gamma_c > \gamma_{tvp}$, where $u_N^*$ is the normalized $u$ after $N$ cycles of constant $\gamma_c$ and $\gamma_{tvp}$ is the practical $\gamma_{tv}$.

(b) The model should be capable of predicting both positive and negative $u$ at cyclic strain levels larger than $\gamma_{tvp}$.

(c) The model should be convenient for practical use, *i.e.*, the determination of the parameters should be clear and simple.

(d) Optionally, the model should have a format compatible with the pore water pressure models for sands currently used in 1-D seismic response computer programs, so that it can be easily incorporated in such computer programs.

Since our present knowledge does not allow development of the pore water pressure generation model based on the interparticle forces which govern complex pore water pressure response of clay microstructure, the "curve-fitting" with appropriate definition of coefficients and clearly stated simplifications seems to be the only suitable approach which satisfies all of the above mentioned requirements. An attempt to develop such a model has been made herein (see also Matasović and Vucetic, 1991).

A consistent database, which exhibits all characteristics identified earlier, has been selected to illustrate the procedure for developing the model. It consists of three data sets, *i.e.* three sets of experimentally obtained data points, each for a different $OCR$, as shown in Figs. 6, 7 and 8. Each of the data sets has at least two data groups, *i.e.* groups of data points, which are plotted vertically in these figures. Each data group corresponds to a particular constant value of $\gamma_c$ and it therefore represents the results of a single strain-controlled test. The selected database is given in the digitized form in Table 1.

All of the corresponding cyclic strain-controlled tests were conducted by Vucetic (1988) in the NGI-type constant volume equivalent undrained CyDSS device on "undisturbed" samples of an offshore clay, called the VNP clay. The VNP clay is a blue-gray stiff to medium plastic clay with black traces of organic content and some silt. The water content after consolidation ranged from 41–49%, the liquid limit from 71–93%, and the plasticity

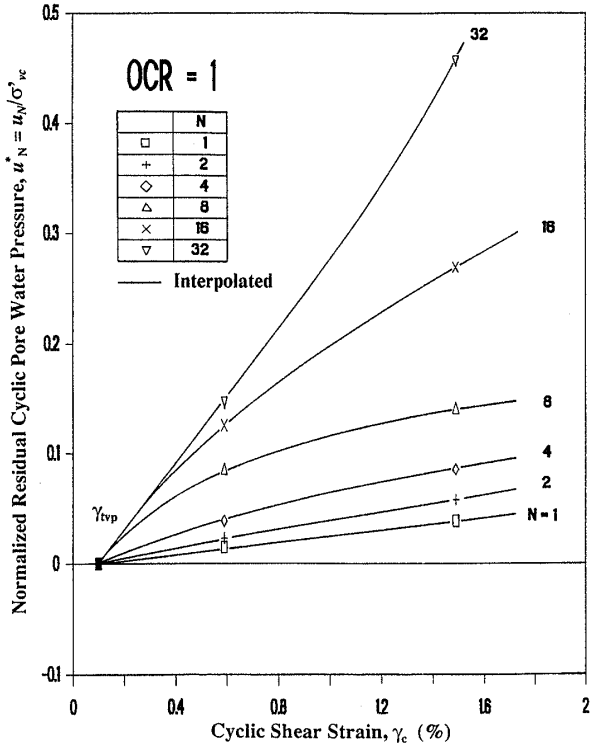


**Fig. 6. Polynomials of second degree interpolated through measured data for $OCR=1$**

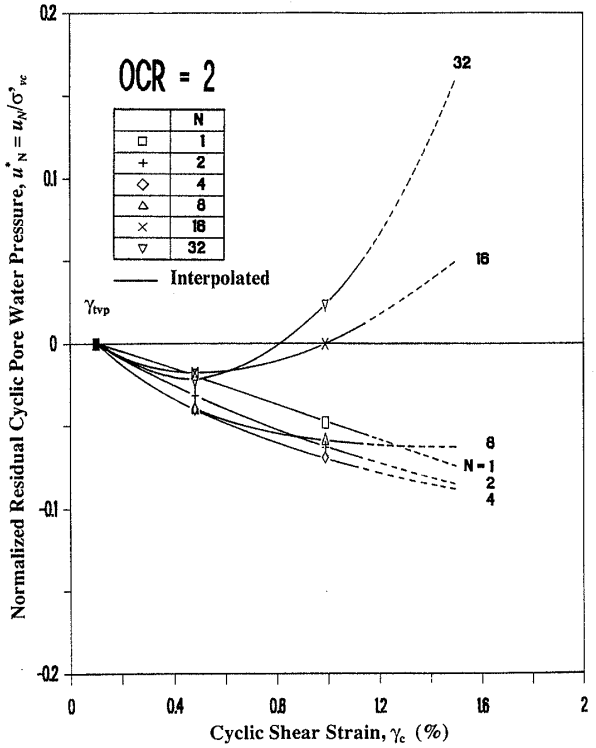


**Fig. 7. Polynomials of second degree interpolated through measured data for $OCR=2$**

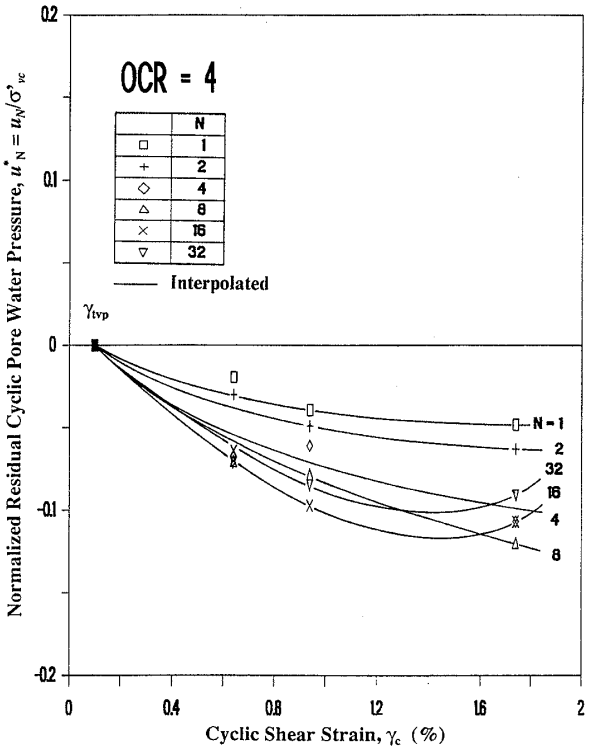


**Fig. 8. Polynomials of second degree interpolated through measured data for $OCR=4$**

ty index, *PI*, was equal to 45±6%. In the plasticity chart, all data points plot along the "A" line. Depending on the actual depth of the sample, the undrained shear strength determined with the pocket torvane before trimming varied between 40 to 90 KPa.

It should be noted that data on $\gamma_{tv}$ are not available from the study by Vucetic (1988), since the existence of $\gamma_{tv}$ in clays has not been considered at that time. Consequently, the practical volumetric threshold shear strain is approximated and assumed here to be a part of the database. The value of $\gamma_{tvp}=10^{-1}\%$ has been selected on the basis of studies by Ohara and Matsuda (1987, 1988) and Chu and Vucetic (1990). This $\gamma_{tvp}$ is included in Table 1 as the points corresponding to $u^*_N=0$ and $\gamma_c=0.10\%$. Thus, the selected database for each pair of $N$ and $OCR$ contains three $u^*_N$ vs. $\gamma_c$ data points, with the exception of the data set 3, which for each pair of $N$ and $OCR$ has 4 data points.

Three points represent a reasonable minimum of data sufficient to describe the pore water pressure generation by the

**Table 1. Database for development of the pore water pressure generation model**

**Set 1** ($OCR=1$; $\gamma_{tvp}=10^{-1}\%$)

| $\gamma_c$ (%) | $u^*_1$ | $u^*_2$ | $u^*_4$ | $u^*_8$ | $u^*_{16}$ | $u^*_{32}$ |
|---|---|---|---|---|---|---|
| 0.10 | 0 | 0 | 0 | 0 | 0 | 0 |
| 0.59 | 0.015 | 0.023 | 0.039 | 0.086 | 0.126 | 0.146 |
| 1.49 | 0.039 | 0.058 | 0.086 | 0.141 | 0.269 | 0.456 |

**Set 2** ($OCR=2$; $\gamma_{tvp}=10^{-1}\%$)

| $\gamma_c$ (%) | $u^*_1$ | $u^*_2$ | $u^*_4$ | $u^*_8$ | $u^*_{16}$ | $u^*_{32}$ |
|---|---|---|---|---|---|---|
| 0.10 | 0 | 0 | 0 | 0 | 0 | 0 |
| 0.48 | −.019 | −.032 | −.040 | −.039 | −.025 | −.019 |
| 0.99 | −.048 | −.063 | −.069 | −.058 | .001 | .023 |

**Set 3** ($OCR=4$; $\gamma_{tvp}=10^{-1}\%$)

| $\gamma_c$ (%) | $u^*_1$ | $u^*_2$ | $u^*_4$ | $u^*_8$ | $u^*_{16}$ | $u^*_{32}$ |
|---|---|---|---|---|---|---|
| 0.10 | 0 | 0 | 0 | 0 | 0 | 0 |
| 0.64 | −.019 | −.030 | −.066 | −.069 | −.063 | −.070 |
| 0.94 | −.039 | −.049 | −.061 | −.078 | −.097 | −.085 |
| 1.74 | −.048 | −.063 | −.107 | −.120 | −.107 | −.091 |

parabola. The parabola through three specified points can be represented by the polynomial of the second degree having the following form:

$$u^*_N=A(\gamma_c-\gamma_{tvp})^2+B(\gamma_c-\gamma_{tvp}) \qquad (1)$$

where:

- $u^*_N$ Normalized cyclic pore water pressure, $u^*_N=u_N/\sigma'_{vc}$
- $\gamma_c$ Cyclic shear strain amplitude
- $\gamma_{tvp}$ Practical volumetric threshold cyclic shear strain
- A, B Functions of $N$ and $OCR$, determined by "best fit" procedure

Equation (1) represents a model which describes the normalized residual pore water pressure generation for a given pair of $N$ and $OCR$ in the range of shear strains between $\gamma_{tvp}$ and the largest $\gamma_c$ in the data set.

In the case of an ideal database, when available data sets are of high quality and consist of 3 measured data points per given pair of $N$ and $OCR$, the polynomials should be constructed directly through the measured points. If the available measured data are not fully consistent, which will depend on the quality of testing (*e.g.* accuracy of measurements, false

deformations, the disturbance and uniformity of specimens), the polynomials should be interpolated through the data points by following general trends of the development of $u$ and using an engineering judgement. A similar approach, of course, also applies for a redundant database, when besides $\gamma_{tvp}$ more than two measured points of $u_N^*$ vs. $\gamma_c$ are available for a given pair of $N$ and $OCR$. In such a case the "best fit" polynomial of the second degree passing through the point ($u_N^*=0$, $\gamma_c=\gamma_{tvp}$) can be interpolated through the measured points, while an error in fitting could be minimized by means of the least square method.

For a given pair of $N$ and $OCR$, A and B in Eq. (1) are dimensionless fitting coefficients. However, if for a given $OCR$ the relationship is broadened to other $N$-s, functional relationships between A and $N$, and B and $N$ can be established. Furthermore, since the relationship for $u_N^*$ also must include different $OCR$-s, the A and B are becoming in their final form functions of $N$ and $OCR$, *i.e.*, $A=f(N, OCR)$ and $B=f(N, OCR)$. The procedure on how to obtain these coefficients of the model, *i.e.*, the functions A and B, follows.

### 5.1 *Determination of the Coefficients*

The families of polynomials of the second degree constructed according to Eq. (1) for fixed $N$-s using data given in Table 1, are shown in Fig. 6 for $OCR=1$, Fig. 7 for $OCR=2$ and Fig. 8 for $OCR=4$. It can be noticed that for $OCR=1$ and 2 the polynomials are constructed directly through the measured data points. However, in the case of $OCR=4$ the measured data are not so consistent because of the manual control of the specimen height (Vucetic, 1988). Also, besides the threshold point, three data points are available for given $N$. Therefore, in this particular case shown in Fig. 8, the polynomials of the second degree are interpolated through the data points according to general trends of the development of $u$.

The discrete values of dimensionless fitting coefficients A and B, which determine families of polynomials shown in Figs. 6 through 8, are plotted in Fig. 9 versus corresponding $N$-s ($N=1$, 2, 4, 8, 16 and 32) for given $OCR$-s. The A vs. $N$ and B vs. $N$ relations for a given $OCR$ can be further "best fitted" by any polynomial having degree, $m$, which is smaller than the total number of discrete points. Thus the functional relationship between A and $N$ and B and $N$ can be expressed in the form:

$$A(N)=\sum_{i=0}^{m} a_i N^i \tag{2}$$

$$B(N)=\sum_{i=0}^{m} b_i N^i, \tag{3}$$

where:

| | |
|---|---|
| $A(N)$, $B(N)$ | "Best fit" functions for the A vs. $N$ and B vs. $N$ relations for a given $OCR$ |
| $N$ | Number of shear straining cycle |
| $a_i$, $b_i$ | Coefficients of functions $A(N)$ and $B(N)$ respectively |
| $m$ | Degree of the "best fit" functions $A(N)$ and $B(N)$. |

Generally, for the database given in Table 1, the value of $m$ which would yield an exact solution, *i.e.*, the curve passing through all given discrete points, is 5. However, in Fig. 9, A vs. $N$ and B vs. $N$ relations are approximated quite well by either polynomial of the second degree ($m=2$) plotted by a dashed curve or the third degree ($m=3$) plotted by a solid curve. In both cases the approximation error was minimized by means of the least square method. From comparison of the dashed and solid curves, it can be seen that the polynomial of the second degree fits the data reasonably well. The only exception is a deviation between two $B(N)$ functions for $OCR=2$. This deviation will be addressed latter.

Once $m$ is selected and the coefficients $a_i$ and $b_i$ for given $OCR$-s are determined, the last step of the determination of functions $A(N, OCR)$ and $B(N, OCR)$ can be performed. This step consists of determining the relations between the coefficients $a_i$ and $b_i$ and $OCR$, *i.e.*, the determination or approximation of the functions $a_i=f_i(OCR)$ and $b_i=f_i(OCR)$. The coefficients $a_i$ and $b_i$ are plotted vs. $OCR$ in Fig. 10. Again, in the same manner as for

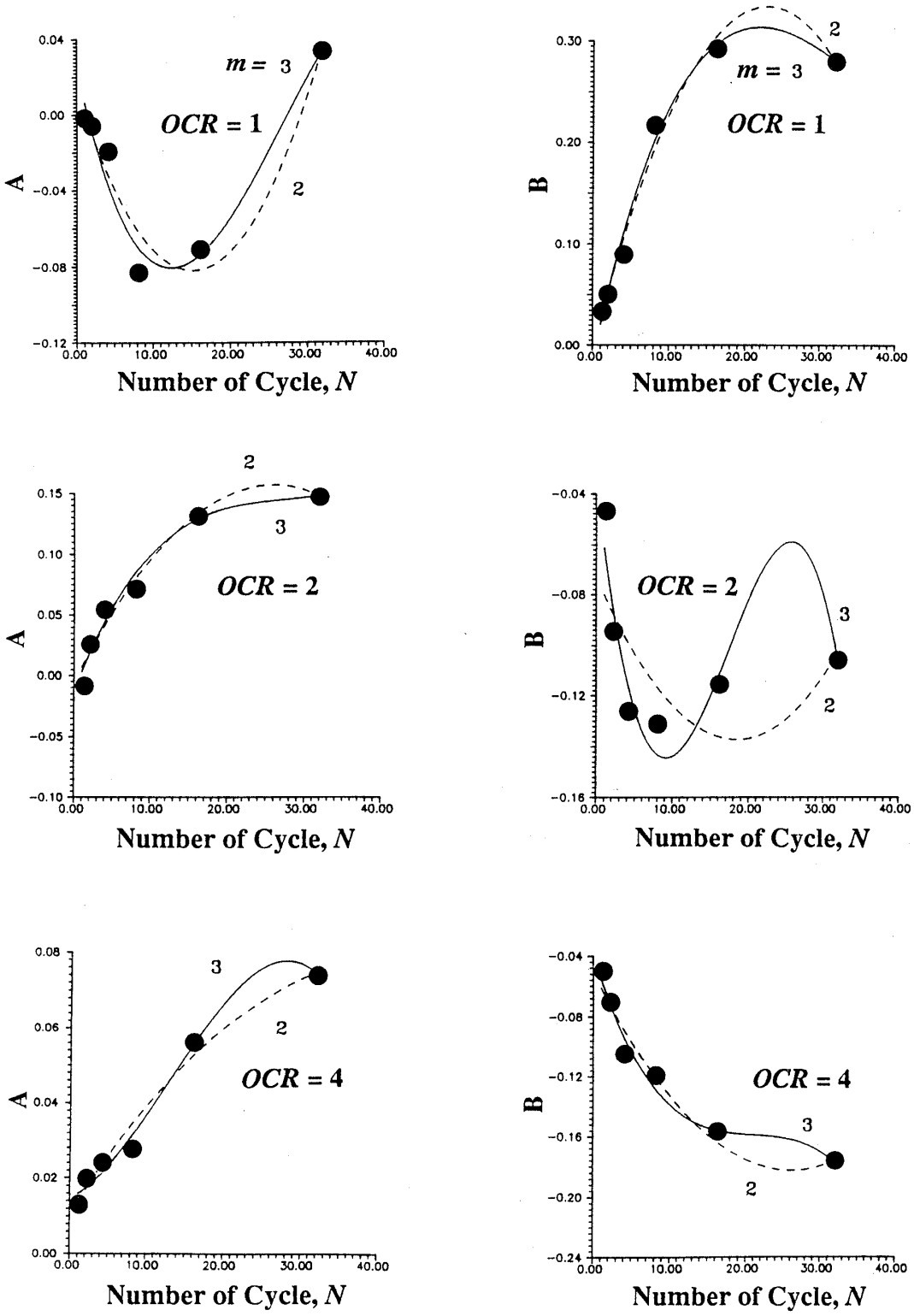


**Fig. 9. Determination of polynomial functions A($N$) and B($N$) for a given *OCR* (Dashed lines, $m=2$; Solid Lines, $m=3$)**

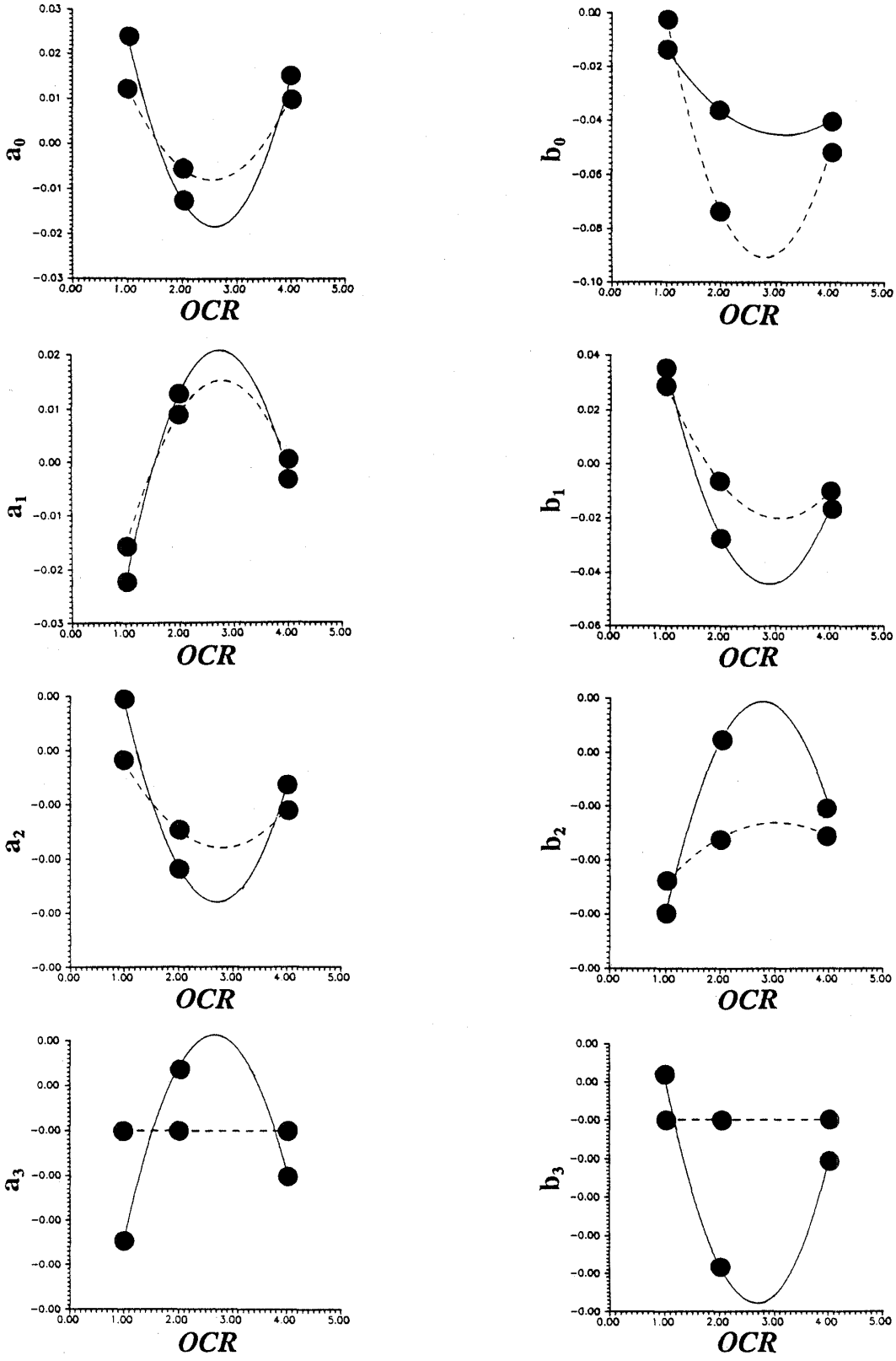


**Fig. 10. Determination of polynomial functions $a_i(OCR)$ and $b_i(OCR)$ for given $m$ and $n$ (Dashed lines, $m=2$ and $n=2$; Solid Lines, $m=3$ and $n=2$)**

the determination of functions A($N$) and B($N$), the following functional relationships can be written:

$$a_i(OCR)=\sum_{j=0}^{n}\alpha_{ij}OCR^j, \quad (4)$$

$$b_i(OCR)=\sum_{j=0}^{n}\beta_{ij}OCR^j, \quad (5)$$

where:

| | |
|---|---|
| $a_i(OCR)$, $b_i(OCR)$ | "Best fit" functions for the $a_i$ vs. $OCR$ and $b_i$ vs. $OCR$ relations |
| $OCR$ | Overconsolidation ratio |
| $\alpha_{ij}$, $\beta_{ij}$ | Coefficients of functions $a_i(OCR)$ and $b_i(OCR)$ respectively |
| $n$ | Degree of the "best fit" functions $a_i(OCR)$ and $b_i(OCR)$. |

In Fig. 10 the "best fit" functions $a_i(OCR)$ and $b_i(OCR)$ are plotted for $n=2$. The dashed and the solid lines in the same figure refer to the cases of the approximation of A vs. $N$ and B vs. $N$. relations by the polynomial of the second degree ($m=2$) and by the polynomial of the third degree ($m=3$) respectively. It should be noticed that the total number of functions $a_i(OCR)$ and $b_i(OCR)$, and the related number of their coefficients $\alpha_{ij}$ and $\beta_{ij}$ depend on $m$, *i.e.*, on the degree of the polynomial used to define A($N$) and B($N$). Thus for the case ($m=2$ and $n=2$), both $a_3(OCR)$ and $b_3(OCR)$ are horizontal straight lines passing through origin with the value of coefficients $\alpha_{3j}$ and $\beta_{3j}$ equal to zero. Using higher degrees of the polynomials (larger $m$ and $n$) will, of course, generally yield a better approximation. However, the use of the larger degrees of the polynomials produces larger amounts of data for manipulations.

For convenience, the coefficients $\alpha_{ij}$ and $\beta_{ij}$ determined for the VNP clay for both cases ($m=2$ and $m=3$) are given in Table 2.

### 5.2 *General Form of the Model*

Equation (1) can be written in the following general form by inserting Eqs. (2) through (5):

$$u_N^*=\sum_{i=0}^{m}N^i\left(\sum_{j=0}^{n}\alpha_{ij}OCR^j\right)(\gamma_c-\gamma_{tvp})^2 + \sum_{i=0}^{m}N^i\left(\sum_{j=0}^{n}\beta_{ij}OCR^j\right)(\gamma_c-\gamma_{tvp}). \quad (6)$$

For the VNP clay the cyclic pore water pressure model can be obtained by inserting the coefficients from Table 2 into the Eq. (6). It should be mentioned that these coefficients are determined by means of a commercially available software package. The graphical output that accompanies application of the

**Table 2. Coefficients $\alpha_{ij}$ and $\beta_{ij}$ for the VNP Clay**

**Case ($m=2$; $n=2$)**

| | $\alpha_{ij}$ | | | $\beta_{ij}$ | | |
|---|---|---|---|---|---|---|
| | j=0 | j=1 | j=2 | j=0 | j=1 | j=2 |
| i=0 | .0478668 | −.0439187 | .0086286 | .1244726 | −.1537943 | .0274584 |
| i=1 | −.0570942 | .0545026 | −.0098521 | .0885899 | −.0708699 | .0115547 |
| i=2 | .0015635 | −.0014034 | .0002507 | −.0020174 | .0016531 | −.0002752 |
| i=3 | 0 | 0 | 0 | 0 | 0 | 0 |

**Case ($m=3$, $n=2$)**

| | $\alpha_{ij}$ | | | $\beta_{ij}$ | | |
|---|---|---|---|---|---|---|
| | j=0 | j=1 | j=2 | j=0 | j=1 | j=2 |
| i=0 | .0946990 | −.0870851 | .0167719 | .0244832 | −.0446506 | .0071284 |
| i=1 | −.0822668 | .0777049 | −.0142292 | .1423350 | −.1295360 | .0224823 |
| i=2 | .0038419 | −.0035035 | .0006468 | −.0068819 | .0069630 | −.0012643 |
| i=3 | −.0000482 | .0000444 | −.0000084 | .0001029 | −.0001123 | .0000209 |

package helps in making decisions on acceptable approximations in each step of the procedure. It should be also mentioned that the whole procedure of coefficients determination can be readily programmed as a single subroutine with an input in terms of $u_N^*$ vs. $\gamma_c$ as listed in Table 1. However, in that case the control of the quality of the approximations might be lost.

## 6. ANALYSIS

The analysis presented herein consists of two steps. In the first step it is determined whether Eq. (6) can yield acceptable results for the approximation case ($m=2$, $n=2$), or whether the approximation by the higher degree of the polynomial, *i.e.*, case ($m=3$, $n=2$) is necessary. In the second step, interpolation for $OCR=1.4$ is performed and the analytical curves are compared to the corresponding experimental data obtained independently.

The $u_N^*$ vs. $\gamma_c$ curves calculated for $OCR$-s 1, 2 and 4 using Eq. (6) and coefficients for case ($m=2$, $n=2$) (see Table 2) are compared with measured data in Figs. 11, 12 and 13. For the case ($m=3$, $n=2$) the same comparison is shown in Figs. 14, 15 and 16. A careful examination of the agreement between calculated curves and measured data reveals that it is not completely satisfactory in Fig. 12 for $OCR=2$ and ($m=2$, $n=2$) and perhaps in Fig. 13 for $OCR=4$ and ($m=2$, $n=2$). It should be noticed that the unsatisfactory agreement for $OCR=2$ is congruent with the discrepancy shown in Fig. 9 for B($N$) curve for $m=2$ corresponding to $OCR=2$. Also, from the form of Eq. (1) it can be noticed that B($N$) influences the results more when $(\gamma_c-\gamma_{tvp})<1$, which is consistent with the discrepancies at small strains in Fig. 12.

It can be concluded that, although for the NC clay ($OCR=1$) there is no major difference between the two approximation cases, when the behavior of the OC clay is modelled, the approximation by the polynomial of higher degree might be necessary for satisfactory agreement between measured and calculated results. Therefore, only the approximation

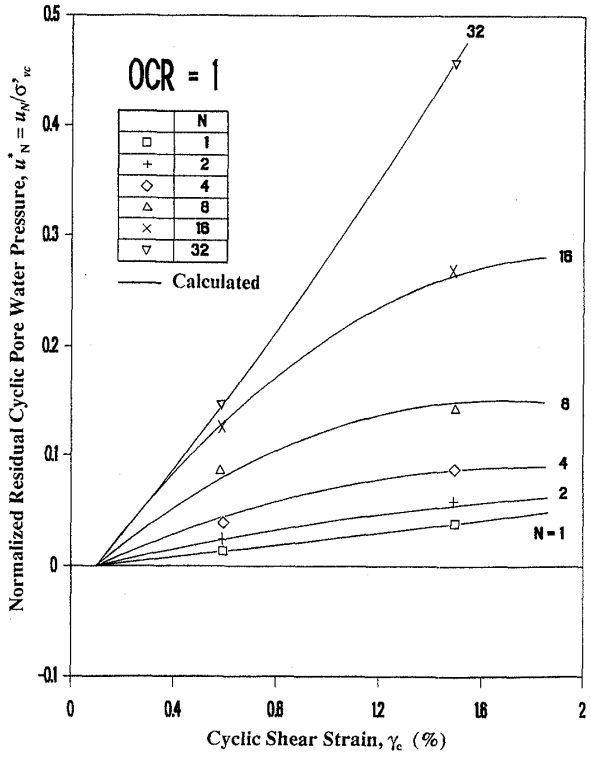


**Fig. 11. Normalized cyclic pore water pressure variation curves calculated for $OCR=1$ using $m=2$ and $n=2$**

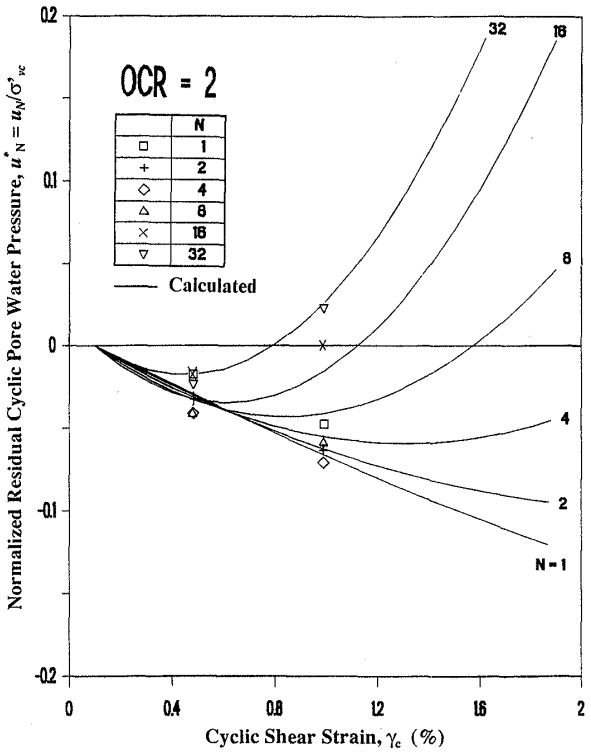


**Fig. 12. Normalized cyclic pore water pressure variation curves calculated for $OCR=2$ using $m=2$ and $n=2$**

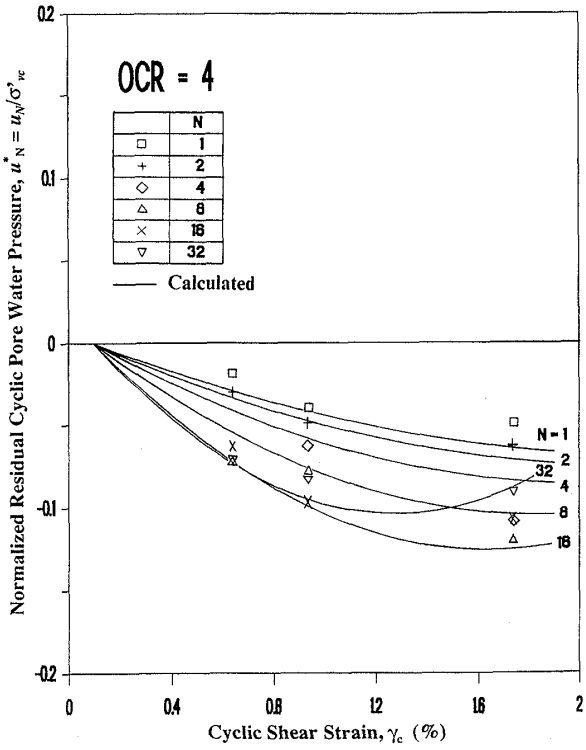


Fig. 13. Normalized cyclic pore water pressure variation curves calculated for $OCR=4$ using $m=2$ and $n=2$

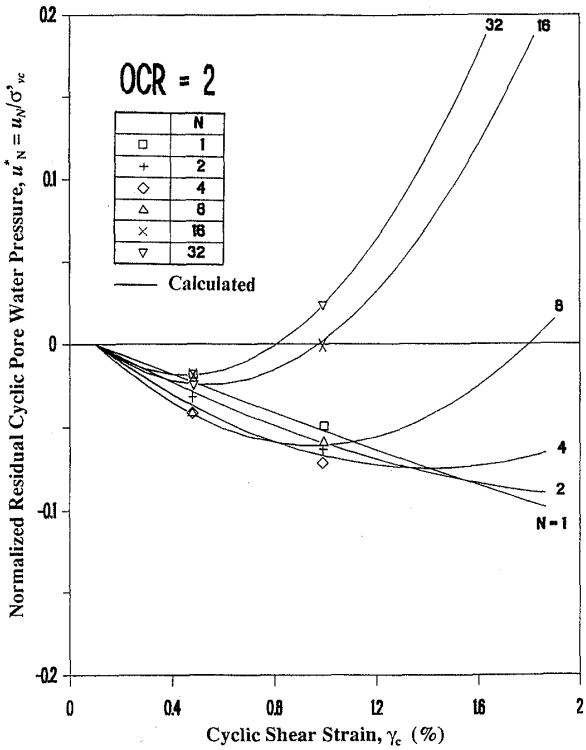


Fig. 15. Normalized cyclic pore water pressure variation curves calculated for $OCR=2$ using $m=3$ and $n=2$

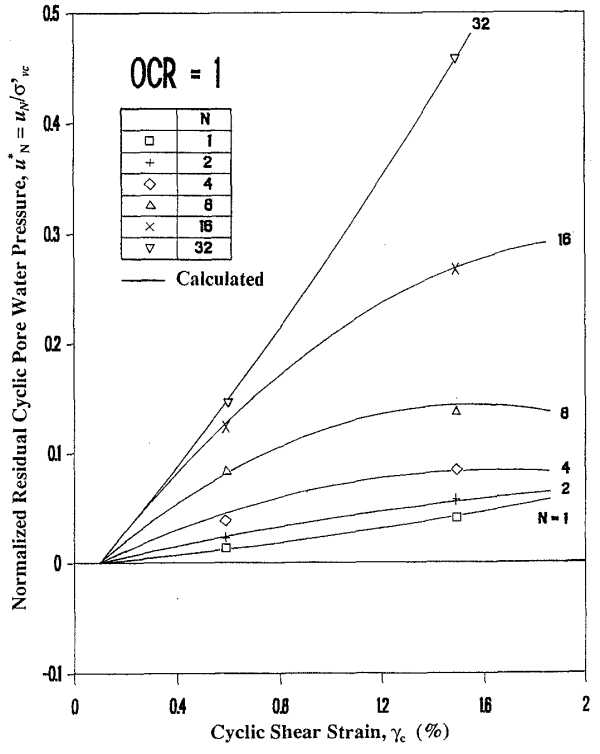


Fig. 14. Normalized cyclic pore water pressure variation curves calculated for $OCR=1$ using $m=3$ and $n=2$

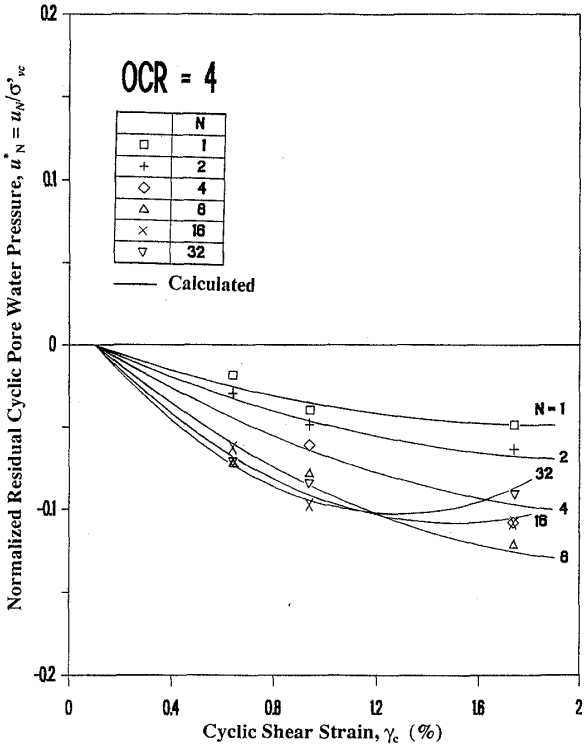


Fig. 16. Normalized cyclic pore water pressure variation curves calculated for $OCR=4$ using $m=3$ and $n=2$

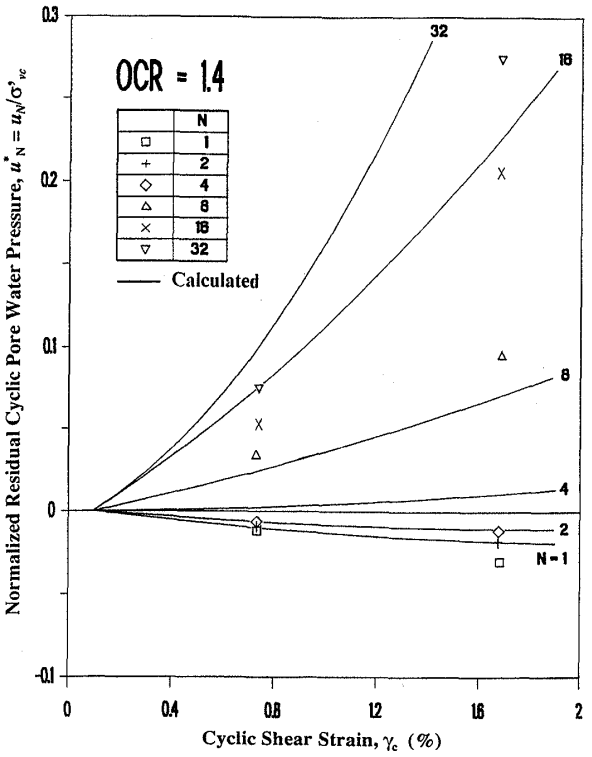


**Fig. 17. Comparison between calculated and measured data for $OCR=1.4$ and $m=3$ and $n=2$**

case ($m=3$, $n=2$) is used here to verify whether the model can be used for the prediction of $u_N^*$ for $OCR$-s different than those included in the database, *i.e.*, different than those originally used for the development of the model.

The interpolation is performed here for the $OCR=1.4$. The VNP clay was independently tested at this particular $OCR$ (Vucetic, 1988). The experimental data are compared to the results of the interpolation performed by Eq. (6) in Fig. 17. A proper pore water pressure generation trend between the calculated and measured data can be seen. The direct agreement between the calculated and measured results, though not perfect, is reasonable. Accordingly, Fig. 16 further confirms that the phenomenon of the residual pore water pressure generation by cyclic shear straining can be described in a satisfactory manner by the proposed phenomenological model.

## 7. DISCUSSION AND CONCLUSIONS

A model for the generation of residual cyclic pore water pressure in clay is presented. The model directly encompasses negative residual cyclic pore water pressures which may develop in overconsolidated clays. The model is applied to the results of the NGI-type CyDSS constant volume equivalent undrained tests performed on an offshore clay. The tests were conducted in a cyclic strain-controlled mode, *i.e.*, by applying the constant cyclic shear strain amplitude, $\gamma_c$. The model is therefore applicable to such a cyclic strain-controlled condition. Because of its general form, the model can be also applied to the results of the cyclic strain-controlled triaxial and hollow cylinder tests.

The development of the residual cyclic pore water pressure after cycle $N$, $u_N$, which depends primarily on $\gamma_c$, $N$ and $OCR$ is expressed in the model in the normalized form with respect to the vertical effective consolidation stress $\sigma'_{vc}$, *i.e.*, in the form of $u_N^*=u_N/\sigma'_{vc}$. An important component incorporated into the model is the practical volumetric threshold shear strain, $\gamma_{tvp}$, below which no significant pore water pressures develop. Accordingly, the model describes $u_N^*$ as a function of $\gamma_c$, $N$, $OCR$ and $\gamma_{tvp}$, *i.e.*, $u_N^*=f(\gamma_c, N, OCR, \gamma_{tvp})$.

The model is developed by a systematic curve fitting technique. In other words, it describes the cyclic loading effects without expressing them in terms of some fundamental material laws. The presented model is therefore a phenomenological model. Until the microstructural mechanisms which govern the generation of $u$, including the negative $u$ which develops in overconsolidated clays, are fully explained, the curve fitting approach used in this study seems to be the most appropriate way to describe the phenomenon.

The interpolations carried out in this study reveal that the model is suitable for practical applications, *i.e.*, it is convenient enough to be incorporated into finite element programs for 1-D seismic site response. If the database for the determination of coefficients of the model is small or, when extrapolation of $u_N^*$ values for $\gamma_c$, $N$ and $OCR$ much larger than those included in the database is needed, an engineering judgement should be used when applying the model.

## 8. ACKNOWLEDGMENTS

The research reported herein was supported by the National Science Foundation Grants No. MSS-9012975 and MSS-8922170. This support is gratefully acknowledged. Mr. D. Spisic from the Department of Mathematics at University of California, Los Angeles, provided useful discussions on mathematical aspects of the model.

## REFERENCES

1) Andersen, K. H., Pool, J. H., Brown. S. F. and Rosenbrand, W. F. (1980): "Cyclic and static laboratory tests on Drammen clay," Journal of the Geotechnical Engineering Division, Proc. ASCE, Vol. 106, No. GT5, pp. 499–529.
2) Azzouz, A. S., Malek, A. M. and Baligh, M. M. (1989): "Cyclic behavior of clays in undrained simple shear," Journal of the Geotechnical Engineering Division, Proc. ASCE, Vol. 115, No. 5, pp. 637–657.
3) Chu, H.-H. and Vucetic, M. (1990): "Settlement of a compacted clay in a cyclic direct simple shear device," ASTM Geotechnical Testing Journal, Vol. 15, No. 4. (December).
4) Dobry, R. and Swiger, W. F. (1979): "Threshold strain and cyclic behavior of cohesionless soils," Proc. 3rd ASCE/EMDE Specialty Conference, Austin, Texas, pp. 521–525.
5) Dobry, R., Powell, D., Yokel, F. Y. and Ladd, R. S. (1980): "Liquefaction potential of saturated sand—The stiffness method," Proc. 7th World Conference on Earthquake Engineering, Istanbul, Turkey, Vol. 3, pp. 25–32.
6) Dobry, R., Ladd, R. S., Yokel, F. Y., Chung, R. M. and Powell, D., (1982): "Prediction of pore water pressure buildup and liquefaction of sands during earthquakes by the cyclic strain method," Building Science Series 183, National Bureau of Standards, U.S. Department of Commerce, U.S. Government Printing Office, Washington, D.C.
7) Dobry, R., Pierce, W. G., Dyvik, R., Thomas, G. E. and Ladd, R. S. (1985): "Pore pressure model for cyclic straining of sand," Research Report, Civil Engineering Department, Rensselaer Polytechnic Institute, Troy, New York, 56 pp.
8) Dobry, R. and Vucetic, M. (1987): "Dynamic properties and seismic response of soft clay deposits," State-of-the Art Paper, Proc. International Symposium on Geotechnical Engineering of Soft Soils, Mexico City, Mexico, Vol. 2, pp. 51–87.
9) Finn, W. D. L. and Bhatia, S. K. (1981): "Prediction of seismic porewater pressures," Proc. 10th International Conference on Soil Mechanics and Foundation Engineering, Stockholm, Vol. 3, pp. 201–206.
10) Kvasnicka, P. and Ivsic, T. (1991): "Presentation of the porewater pressure buildup using Moroto's and state parameter," Proc. 2nd International Conference on Recent Advances in Geotechnical Earthquake Engineering and Soil Dynamics, St. Louis, Missouri, pp. 171–174.
11) Matasović, *N.* and Vucetic, M. (1991): "Modelling of the residual pore water pressure in clay generated by cyclic shear straining," Research Report, Civil Engineering Department, University of California, Los Angeles, California, 58 pp.
12) Matsuda, H., Hoshiyama, E. and Ohara, S. (1991): "Settlement calculations of clay layers induced by earthquake," Proc. 2nd International Conference on Recent Advances in Geotechnical Earthquake Engineering and Soil Dynamics, St. Louis, Missouri, pp. 473–479.
13) Matsui, T., Ohara, H. and Ito, T. (1980): "Cyclic stress-strain history and shear characteristics of clay," Journal of the Geotechnical Engineering Division, Proc. ASCE, Vol. 106, No. GT10, pp. 1101–1120.
14) Moroto, *N.* (1986): "Unique representation of pore pressure developed in cyclic shear for sand in terms of $S_m$ parameter," Proc. JSSMFE Symposium on Cyclic Shear Tests of Soils pp. 125–130 (in Japanese).
15) NGI (1975): Research Project, Repeated Loading on Clay, Summary and Interpretation of Test Results. Report 74037-9, Norwegian Geotechnical Institute, Oslo, Norway.
16) NRC (1985): Liquefaction of Soils During Earthquakes. National Research Cauncil, Committee on Earthquake Engineering, Washington, DC.
17) Ohara, S., Matsuda, H. and Kondo, Y. (1984): "Cyclic simple shear tests on saturated clay with drainage," Proc. Japan Society of Civil Engineers, Vol. 352, pp. 149–158 (in Japanese).
18) Ohara, S. and Matsuda, H. (1987): "Settlement of saturated clay layer induced by cyclic shear," Proc. 9th Southeast Asian Geotechnical Conference, Bangkok, Thailand, pp. 7-13–7-22.
19) Ohara, S. and Matsuda, H. (1988): "Study on settlement of saturated clay layer induced by cyclic shear," Soils and Foundations, Proc. JSSMFE, Vol. 28, No. 3, pp. 103–113.
20) Pyke, R., Seed, H. B. and Chan, C. K. (1975): "Settlement of sands under multi-directional shaking," Journal of the Geotechnical Engineering Division, Proc. ASCE, Vol. 101, No. GT4, pp. 379–398.
21) Seed, H. B. (1979): "Soil liquefaction and cyclic mobility evaluation for level ground during earthquakes," Journal of the Geotechnical Engineering Division, Proc. ASCE, Vol. 105, No. GT2, pp. 201–256.
22) Silver, M. L. and Seed, H. B. (1971): "Volume changes in sands during cyclic loading," Journal of the Soil Mechanics and Foundations Division, Proc. ASCE, Vol. 97, No. SM9, pp. 1171–1182.
23) Stoll, R. D. and Kald, L. (1977): "Treshold of dilation under cyclic loading," Technical Note, Journal of the Geotechnical Engineering Division, Proc.

ASCE, Vol. 103, No. GT10, pp. 1174–1178.
24) Tan, K. and Vucetic, M. (1989): "Behavior of medium and low plasticity clays under cyclic simple shear conditions," Proc. 4th International Conference on Soil Dynamics and Earthquake Engineering, Mexico City, Mexico, pp. 131–142.
25) Towhata, I. and Ishihara, K. (1985): "Shear work and pore water pressure in undrained shear," Soils and Foundations, Proc. JSSMFE, Vol. 25, No. 3, pp. 73–84.
26) Vucetic, M., Dobry, R., Petrakis, E. and Thomas, G. E. (1985): "Cyclic simple shear behavior of overconsoildated offshore clay," Proc. 2nd International Conference on Soil Dynamics and Earthquake Engineering, on board of the liner, the Queen Elizabeth 2, pp. 2-107–2-116.
27) Vucetic, M. (1988): "Normalized behavior of offshore clay under uniform cyclic loading," Canadian Geotechnical Journal Vol. 25, pp. 33–41.
28) Vucetic, M. (1991): "Relation between the basic soil properties and seismic response of natural soil deposits," Proc. International Symposium on Building Technology and Earthquake Hazard Mitigation, City of Kunming, People's Republic of China, pp. 252–267.
29) Youd, L. T. (1972): "Compaction of sands by repeated shear straining," Journal of the Soil Mechanics and Foundations Division, Proc. ASCE, Vol. 98, No. SM7, pp. 709–725.

## NOTATION

*Symbols*

| | |
|---|---|
| $a_i$ | Polynomial function |
| A | Polynomial function |
| $b_i$ | Polynomial function |
| B | Polynomial function |
| $D_r$ | Relative density |
| $e$ | Void ratio |
| $m$ | Degree of the polynomial functions A and B |
| $n$ | Degree of the polynomial functions $a_i$ and $b_i$ |
| $N$ | Number of loading or shear straining cycle |
| $OCR$ | Overconsolidation ratio |
| $PI$ | Plasticity index |
| $u$ | Residual cyclic pore water pressure |
| $u^*$ | Normalized $u$; $u^*=u/\sigma'_{30}$ |
| $u_N$ | Residual cyclic pore water pressure after cycle $N$ |
| $u_N^*$ | Normalized $u_N$; $u_N^*=u_N/\sigma'_{vc}$ |
| $\alpha_{ij}$ | Coefficient |
| $\beta_{ij}$ | Coefficient |
| $\gamma_c$ | Cyclic shear strain amplitude |
| $\gamma_{tv}$ | Volumetric threshold cyclic shear strain |
| $\gamma_{tvp}$ | Practical $\gamma_{tv}$ below which no significant $u$ develops |
| $\Delta e$ | Void ratio change |
| $\varepsilon_c$ | Cyclic axial strain amplitude |
| $\sigma'_{30}$ | Effective confining pressure |
| $\sigma'_{vc}$ | Vertical effective consolidation stress |
| $\tau_c$ | Cyclic shear stress amplitude |
| $\tau_{tv}$ | Volumetric threshold cyclic shear stress |

*Abbreviations*

| | |
|---|---|
| CyDSS | Cyclic Direct Simple Shear (test) |
| NC | Normally Consolidated |
| NGI | Norwegian Geotechnical Institute |
| NRC | National Research Council |
| OC | Overconsolidated |
| VNP | Venezuelan North of Paria (offshore clay used in analyses) |
| 1-D | One dimensional |